

Measuring Protein Secretions from Individual Live Cells

M.P. Raphael,¹ J.A. Christodoulides,¹ J.B. Delehanty,² J.P. Long,³ P.E. Pehrsson,³ and J.M. Byers¹

¹Materials Science and Technology Division

²Center for Bio/Molecular Science and Engineering

³Chemistry Division

Introduction: Wounded warriors recovering from blast injuries face wound healing challenges rarely encountered within the civilian population. The need to reconstruct an individual's muscle, skin, or bone on a massive scale has pushed the boundaries of our understanding of the biological signaling that underlies the healing process. Even the healing of a simple cut is an incredibly complex endeavor. The surrounding cells must reconstruct layers of skin, which contain numerous components such as pores and nerve endings, while simultaneously protecting against infection. While it is generally known that this reconstruction process is orchestrated by the cellular secretion of proteins as signaling molecules, very little is understood about how cells organize these secretions in space and time.

This gap in our understanding has its origins in the dominant technique for detecting cell secretions, which is based upon fluorescent labeling. The introduction of these labels necessarily halts or ends an experiment; therefore, the labels are introduced only after a cell has been secreting for hours or days. Using such techniques, any variations in cellular secretions that are on the order of minutes or seconds cannot be detected, leaving an incomplete picture of how cells regulate their secretions throughout the wound healing process. To address this roadblock, we have developed a label-free technique based upon nanoplasmonic imaging that enables the measurement of individual cell secretions with time resolutions below one second. Using this technique, we have captured real-time measurements of antibody secretions from individual hybridoma cells.

Nanoplasmonic Sensors: Arrays of gold nanostructures are fabricated on glass coverslips by electron-beam lithography using NRL's state-of-the-art facilities at the Institute for Nanoscience. The bases of the nanostructures are circular in cross section with diameters of 70 ± 5 nm and heights of 75 ± 2 nm (Fig. 1(a) inset). Each square array typically consists of 400 nanostructures with a spacing of 400 nm between nanostructures. The gold nanostructures are functionalized with a peptide sequence called c-myc, which has a particularly high binding affinity for the antibodies secreted by the hybridoma cells. Nanoplasmonic biosensing is founded upon the fact that the plasmonic resonance of the gold nanostructures exhibits both a red shift and

an increase in scattering intensity when the binding of proteins such as antibodies creates small perturbations in the local index of refraction (Fig. 1(b)).¹ When imaged on a CCD camera, these spectroscopic signatures are manifested as an increase in the brightness of the nanostructures and can be quantified in terms of the local concentration of secreted protein.²

The processed chips are loaded onto an inverted microscope that is enclosed within an environmental chamber designed for live cell studies (Fig. 1(a)). The cells are introduced microfluidically and settle about the arrays (Fig. 1(d)). In addition to monitoring the nanoplasmonic sensors for cell secretions, the design also incorporates a mode from transmitted light illumination for visualizing the cells (Fig. 2(a)) and a fluorescence mode for imaging intracellular fluorescent labels (Fig. 2(c)).

Single Cell Secretions: The real-time measurements on live cells enabled us to observe sudden bursts of antibody secretions as they diffused outwardly from the cell (Fig. 2(b)). The bursts were highly concentrated and corresponded with cell contractions that lasted only about a minute. The size and the slope of the signal were greatest at the array nearest the cell and decreased with increasing distance between cell and array, consistent with a pulsed wave of antibodies originating at the cell and diffusing outward. We also have observed a wide range of continuous secretion rates (Fig. 3(a)), raising the intriguing possibility of linking these secretion rates with the internal state of the cell. From the continuous secretion measurements, we determined the local concentration of antibodies at the sensing arrays closest to the cell (Fig. 3(b)) and from the bursts, we estimated the diffusion constant of the secreted antibodies through the media.

Looking Ahead: The technique presented here describes a methodology for quantitative single cell secretion measurements with unprecedented spatial and temporal resolution and is applicable to almost any cell type. This technique promises to be an enabling technology, providing new insights into how cells signal and coordinate with one another to heal wounds.

[Sponsored by the NRL Institute for Nanoscience]

References

- ¹ M.P. Raphael et al., "A New Methodology for Quantitative LSPR Biosensing and Imaging," *Anal. Chem.* **84**, 1367–1373 (2012).
- ² M.P. Raphael et al., "Quantitative LSPR Imaging for Biosensing with Single Nanostructure Resolution," *Biophys. J.* **104**, 30–36 (2013).

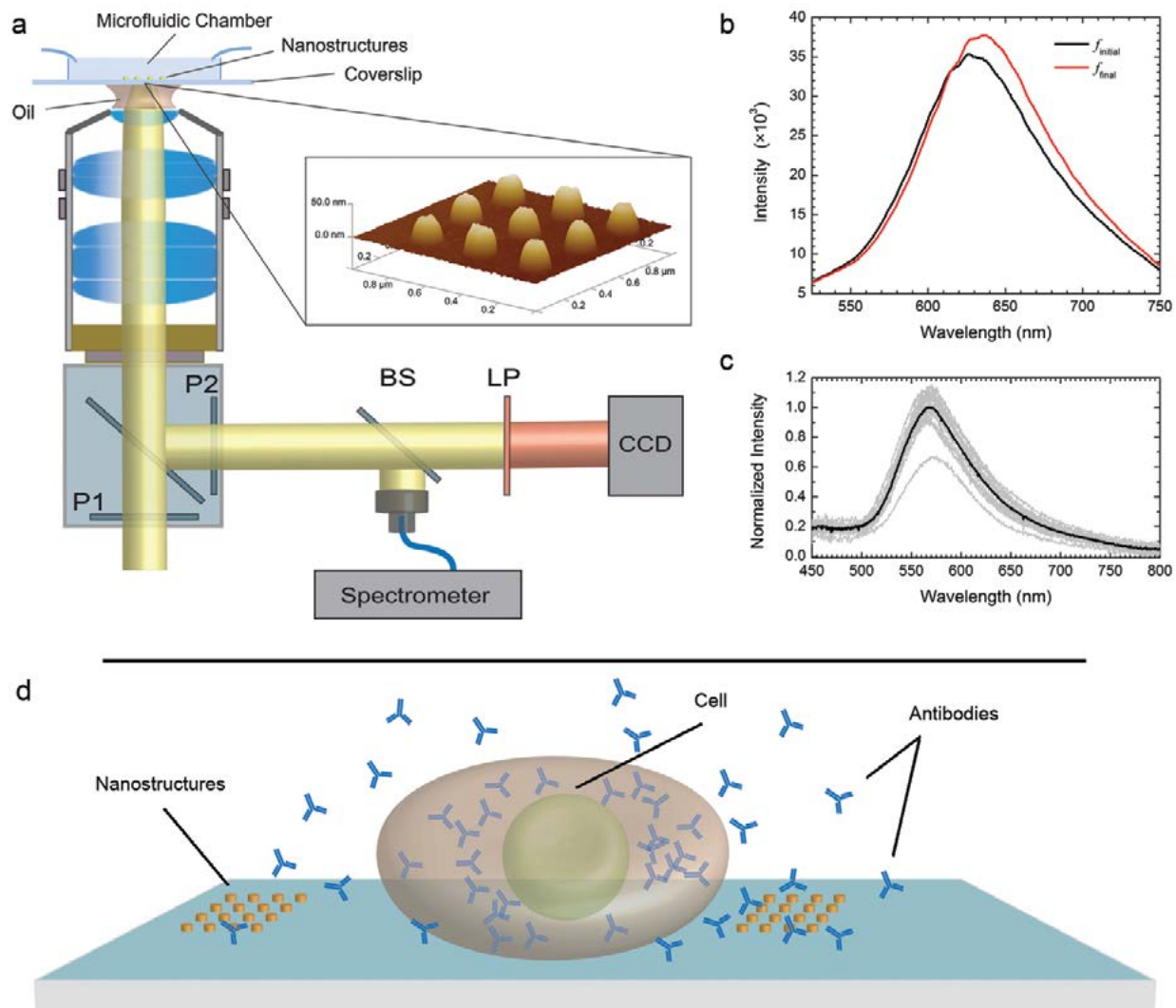


FIGURE 1

(a) Imaging and spectroscopy setup in which P1 and P2 are crossed polarizers, BS is a 50/50 beam splitter, and LP is a long pass filter. The inset shows an atomic force microscope (AFM) scan of a typical array. (b) Two spectra from a specific-binding study in which 200 nM of anti-c-myc was introduced over the c-myc functionalized array. The $f_{initial}$ spectrum (black) was taken before the anti-c-myc was introduced and the f_{final} spectrum (red) after one hour of exposure. (c) Normalized spectra from 18 individual nanostructures taken in air on a separate dark-field microspectroscopy setup. Individual spectra are superposed (gray curves) and compared to the ensemble average (black curve). (d) Illustration of an antibody-secreting cell in registry with nanoplasmonic arrays.

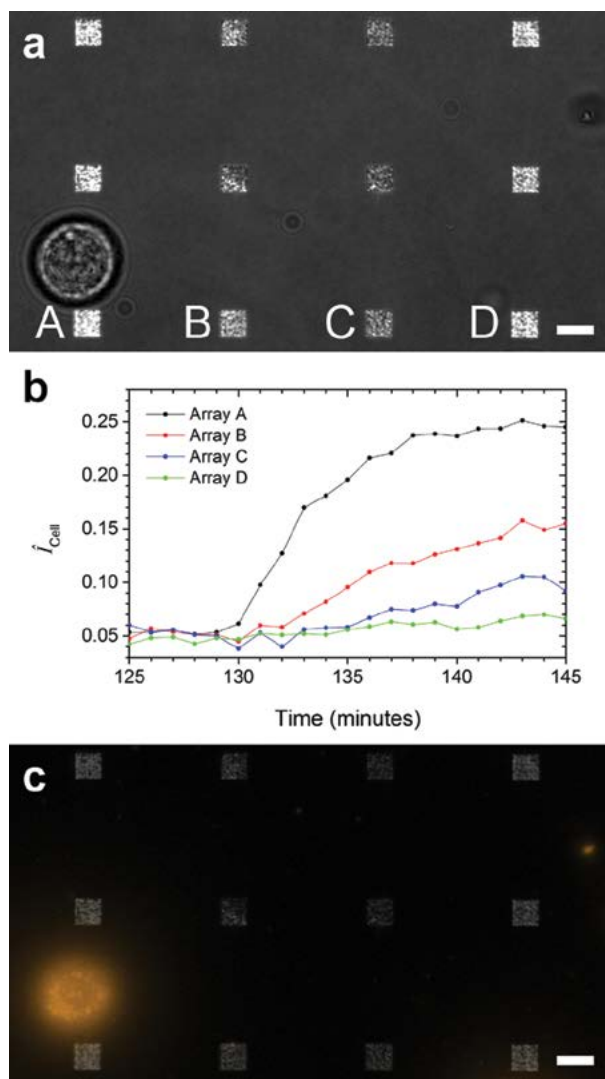


FIGURE 2
 Secretion burst from a single cell (a) Overlay of transmitted light and LSPR images highlights the location of the cell relative to 12 arrays. (b) Normalized LSPR image intensity of four arrays (A-D). The distances from the center of the cell to the center of each array were 15.4 μm , 39.2 μm , 72.2 μm , and 106 μm for Arrays A, B, C and D, respectively. (c) Overlay of LSPR and false-color fluorescence images exposing fluorescently labeled portions of the cell membrane. Scale bar: 10 μm .

A Micromechanical Analogue to Optical Lasers

M.W. Pruessner,¹ J.B. Khurgin,² T.H. Stievater,¹ and W.S. Rabinovich¹

¹Optical Sciences Division

²Johns Hopkins University

Introduction: The force exerted by light is small and generally insignificant. However, optical forces can

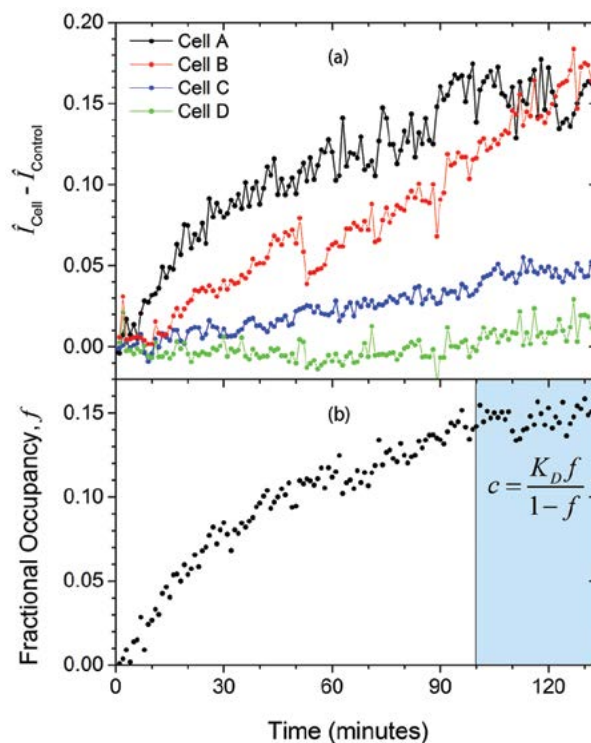


FIGURE 3
 (a) Comparison of the time-dependent secretions from four cells, all of which were within 15 μm of an array. The normalized LSPR image intensity of the array (\hat{I}_{cell}) minus the normalized intensity of a control array (\hat{I}_{control}) is plotted versus time. (b) The fractional occupancy, f , of the closest array to the cell as determined from the LSPR spectra which was collected simultaneously with the LSPR imagery. A concentration of $c = 312 \pm 53$ pM was calculated using the data in the highlighted region at which f was constant with time. K_D is the equilibrium dissociation constant.

have a profound influence on micro/nanomechanical devices. Cavity optomechanics¹ is an exciting multidisciplinary field that exploits these forces by enhancing light-matter interactions via feedback. Here, we report a new approach for exploiting optomechanical forces in a silicon chip-scale integrated device.² We measure a characteristic threshold beyond which the structure's mechanical resonance linewidth collapses and the oscillation amplitude increases sharply — in effect an optically driven mechanical oscillator that displays a striking resemblance to a mechanical “laser”.³ Our structure enables narrow mechanical linewidth micro-

oscillators for applications such as sensing and communications in tomorrow's Navy.

Chip-Scale Micro-Optomechanical Structure:

The device features a silicon waveguide optical microcavity coupled to a microbridge mechanical oscillator, as shown in Fig. 4.² Our unique approach allows independent control of the optical and mechanical parameters, enabling simplified device design. The silicon-based architecture implies the potential for dense chip-scale integration with the capability for mass fabrication in existing silicon foundries.

The optical cavity consists of two grating mirrors. One mirror is fixed while the other is attached to a suspended microbridge mechanical resonator (Fig. 4). As the microbridge oscillates, the mirror is displaced and tunes the optical cavity response (Fig. 4(b)). In other words, the mechanical structure acts on the opti-

Continuous-wave (CW) laser light is focused onto the device's input waveguide (P_{IN} in Fig. 4(b)) and the optomechanical response is measured at the output (P_{OUT}). The oscillator's motion tunes the cavity by changing its length, which in turn changes the optical wavelength at which the cavity is resonant. The optical power in this cavity depends on whether the input laser beam's wavelength is resonant or not, so that any mechanical displacement modulates P_{OUT} . Therefore, the time-varying component of P_{OUT} is a direct measure of the oscillator response.

We determine the mechanical oscillator spectrum for two different laser wavelengths, leaving all other measurement conditions the same. For one wavelength, the mechanical oscillation exhibits a narrow linewidth and large amplitude (red line in Fig. 5), while for another wavelength, the oscillation frequency is shifted and appears strongly damped with a broadened line-

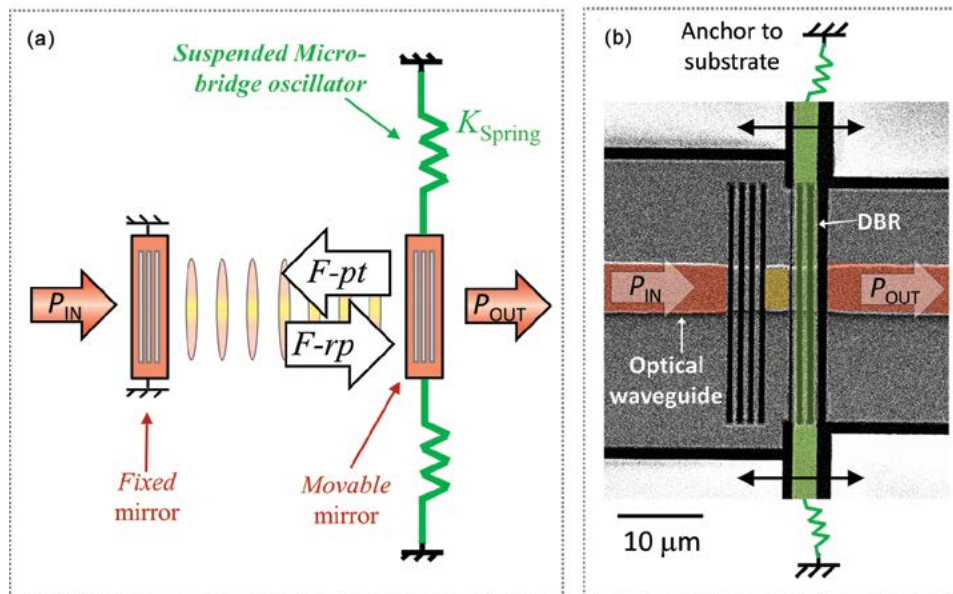


FIGURE 4 (a) Optomechanical device schematic showing an optical cavity consisting of two mirrors (red) and a mechanical oscillator (green). The photothermal ($F-pt$) and radiation pressure ($F-rp$) forces are indicated; (b) scanning electron microscope image of a device fabricated in the NRL Institute for Nanoscience clean room. (DBR = distributed Bragg reflector)

cal structure. Although less intuitive, the optical cavity also affects the mechanical response (“backaction”). Light in the cavity exerts a force on the microbridge, as indicated by $F-pt$ (photothermal force) and $F-rp$ (radiation pressure force) in Fig. 4(a). Therefore, the optical structure also acts on the mechanical structure. This mutual interaction implies a feedback mechanism that we exploit in our measurements.

Mechanical Analog to Optical Laser: The sample is placed in a vacuum cell to minimize air damping.

width (blue line). An analysis shows that the behavior can be explained by feedback optical forces that either amplify or dampen the oscillator's motion,² consistent with observations by other researchers.¹ In particular, we note that the optical forces in Fig. 4(a) act in opposing directions and with vastly different timescales.² The slow photothermal force (microsecond time constant) is responsible for the amplification/damping, while the fast radiation pressure force (picosecond) dominates the frequency tuning. The measurements in Fig. 5 show the profound influence of small optical forces

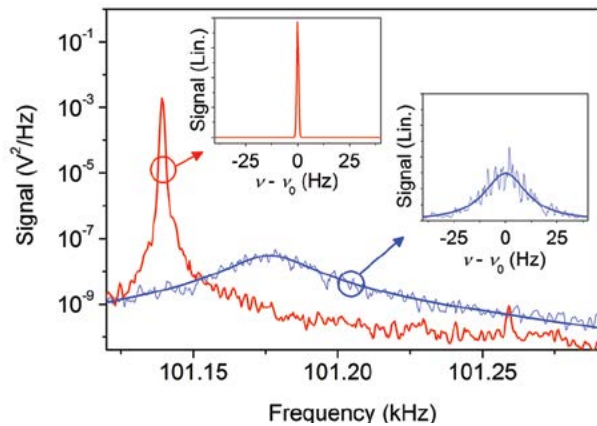


FIGURE 5 Mechanical resonant spectra measured at two different laser wavelengths.² Photothermal (*F-pt*, shown in red) and radiation pressure (*F-rp*, shown in blue) forces change the mechanical oscillators' linewidth, frequency, and vibration amplitude.

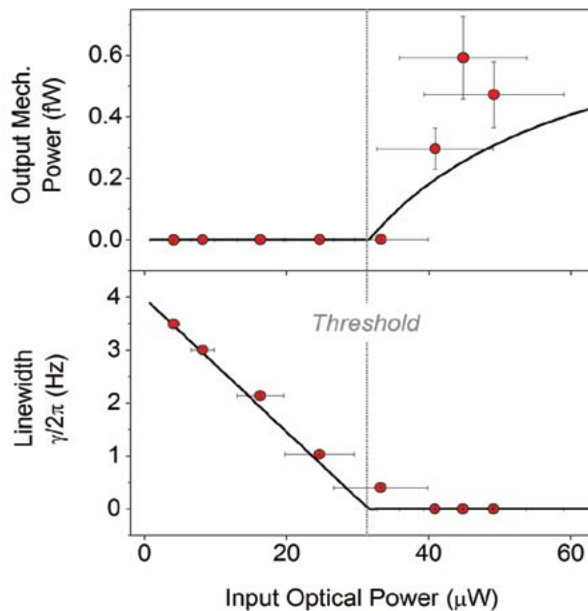


FIGURE 6 Output mechanical power (obtained from the oscillation amplitude) and corresponding linewidth, both measured as a function of input optical power (points: experiment; lines: theory).³

(pico-Newton-level) on micromechanical structures (nanogram-level mass).

Next, we focus on photothermal amplification forces (red line in Fig. 5) by leaving the wavelength and other parameters fixed. We measure the oscillator's vibration amplitude and linewidth as a function of laser power (P_{IN}). The measurements show a strong similarity to the response of an optical laser that is "pumped" with increasing power: (a) a linear decrease in the linewidth, (b) a threshold condition beyond which the linewidth "collapses" (essentially a zero linewidth), and (c) a strong linear increase in oscillation amplitude (mechanical power) beyond threshold (Fig. 6).

Given the similar response between our micromechanical "laser" and a standard optical laser, we develop an optomechanical rate equation theory in analogy to the laser rate equations.³ The theoretical device response shows good agreement with experiments in terms of the mechanical oscillator's output power and linewidth (Fig. 6). Although other groups¹ previously demonstrated a linewidth narrowing as in Fig. 5, our theory is the first to describe this self-oscillation in terms of rate equations with a direct comparison to experiments that clearly exhibit the key characteristics of a laser, namely a threshold condition and linewidth collapse.

Future Directions: Beyond fundamental research our device enables a variety of new sensor applications. First, our approach drives a mechanical resonator to self-oscillation using a single low-power CW laser. Second, the mechanical resonance is monitored using this same laser signal, which has now been modulated by the oscillator motion. Third, the linewidth collapse implies a strong increase in effective $Q_{\text{Mechanical}}$ giving enhanced sensitivity to external perturbations. For example, a chemical sensor may be realized by monitoring the absorption of analytes, which leads to changes in the oscillator mass and frequency. Other future Navy applications include inertial and magnetic field sensors.

Acknowledgments: The authors thank the NRL Institute for Nanoscience staff for clean room access and fabrication assistance. NRL Optical Sciences Division developed the device concept, performed all experiments, and carried out finite element modeling. Johns Hopkins University developed the optomechanical laser rate equation theory and performed calculations.

[Sponsored by the NRL Base Program (ONR) and by ASEE through a Summer Faculty Fellowship]

References

- ¹ T.J. Kippenberg and K.J. Vahala, "Cavity Opto-Mechanics," *Opt. Express* **15**(25), 17172–17205 (2007).
- ² M.W. Pruessner, T.H. Stievater, J.B. Khurgin, and W.S. Rabinovich, "Integrated Waveguide-DBR Microcavity Opto-Mechanical System," *Opt. Express* **19**(22), 21904–21918 (2011).
- ³ J.B. Khurgin, M.W. Pruessner, T.H. Stievater, and W.S. Rabinovich, "Laser-Rate-Equation Description of Opto-Mechanical Oscillators," *Phys. Rev. Lett.* **108**, 223904 (2012).